ISSN 0021-8944, Journal of Applied Mechanics and Technical Physics, 2015, Vol. 56, No. 3, pp. 433–442. © Pleiades Publishing, Ltd., 2015.
Original Russian Text © P. Loganathan, P. Nirmal Chand, P. Ganesan.

TRANSIENT NATURAL CONVECTIVE FLOW OF A NANOFLUID PAST A VERTICAL PLATE IN THE PRESENCE OF HEAT GENERATION

P. Loganathan, P. Nirmal Chand, and P. Ganesan

UDC 536.25; 621.56

Abstract: In this work, an exact analysis on the effects of heat generation and nanoparticle volume concentration on an unsteady free convective flow of a nanofluid past an impulsively started infinite vertical plate is presented. Nanofluids containing nanoparticles of aluminum oxide, copper, titanium oxide, and silver with a nanoparticle volume concentration range smaller than or equal to 0.04 are considered. The governing dimensionless partial differential equations are solved by using the Laplace transform technique. The effects of heat generation and nanoparticle volume concentration on the velocity and temperature profiles are represented graphically. The expressions for the skin friction coefficient and Nusselt number are derived. The effect of heat transfer is found to be more pronounced in a silver–water nanofluid than in the other nanofluids. Comparisons with other published results are found to be in excellent agreement.

Keywords: natural convection, nanofluid, infinite vertical plate, heat generation.

DOI: 10.1134/S002189441503013X

INTRODUCTION

A natural convective flow of a viscous incompressible fluid past a vertical plate has been studied by several researchers due to its potential application in the nuclear reactor cooling system design. In nuclear reactors, the reactor is constructed of several parallel vertical plates with heat generation. Fluid cooling and heating play an important role in many industrial and engineering applications, particularly in nuclear reactors, thin film solar energy collectors, and power generation and transportation. In these applications, the use of common heat transfer fluids, such as water, ethylene glycol, and engine oil, limits heat transfer capabilities due to their poor heat transfer. In many metallurgical processes, such as drawing of continuous filaments through quiescent fluids and annealing of copper wires, the properties of the end product depend greatly on cooling involved in these processes. The lower thermal conductivity of conventional heat transfer fluids is the primary limitation in enhancing the performance and the compactness of many engineering electronic devices.

Nanofluids are nanotechnology-based heat transfer fluids that are derived by stably suspending nanometer-sized particles in conventional heat transfer fluids. A nanofluid is the term first introduced by Choi [1] to describe this new class of nanotechnology-based fluids that exhibit thermal properties superior to those of their host fluids. Nanofluids are found to be devoid of problems such as sedimentation, erosion, and high pressure drop, and a small volume fraction of particles is needed for heat transfer enhancement as compared to microparticle slurries. Nanoparticles used in nanofluids are made of metals (aluminum and copper), carbides, metal oxides, graphite particles, or carbon nanotubes. The base fluid usually is a liquid such as water or ethylene glycol.

Department of Mathematics, Anna University, Guindy, Chennai-600 025, India; logu@annauniv.edu; nimiprasad@yahoo.com; ganesan@annauniv.edu. Translated from Prikladnaya Mekhanika i Tekhnicheskaya Fizika, Vol. 56, No. 3, pp. 105–115, May–June, 2015. Original article submitted May 7, 2013; revision submitted August 12, 2013.

Stokes [2] studied an unsteady flow past an impulsively started infinite plate, which is the fundamental problem in fluid mechanics and heat transfer (Stokes problem). Soundalgekar [3] presented an exact solution for the flow past an infinite isothermal plate impulsively started in a viscous incompressible fluid. The effects of mass transfer and heat sources on the Stokes problem for an infinite vertical plate were studied by Raptis and Tzivanidis [4].

The present study is an extension of the Stokes problem to nanofluids. The phenomenal increase in thermal conductivity of the fluids with an addition of a small volume of nanoparticles created tremendous interest in the technique of heat transfer enhancement. Several researchers [5–8] stated that the thermal conductivity of suspensions can increase by more than 20% with low nanoparticle volume concentrations (1–5 vol.%).

Eastman et al. [9] showed that 60% enhancement of the thermal conductivity can be obtained with a 5 vol.% fraction of CuO nanoparticles in the base fluid (water). The increase in the heat transfer coefficient is a better indicator than the thermal conductivity enhancement for nanofluids used in the design of heat exchange equipment.

Pak and Cho [10] performed experiments on heat transfer in two kinds of nanofluids containing γ-Al_2O_3 and TiO_2 dispersed in water, and the results showed that the Nusselt number of the dispersed fluid increases with increasing volume fraction of suspended solid particles and Reynolds number.

Buongiorno [11] considered seven slip mechanisms that can produce a relative velocity between the nanoparticles and the base fluid and showed that the Brownian diffusion and thermophoresis are important mechanisms in the laminar flow in nanofluids. Wen and Ding [12] studied natural convection in water-based nanofluids containing TiO_2 nanoparticles. Gosselin and Silva [13] showed that there are optimum particle loadings for the highest heat transfer in laminar and turbulent flows of nanofluids. Nanofluid research leads to developing next-generation coolants for numerous engineering and medical applications.

A new theoretical model which predicts strongly particle-size-dependent conductivity was proposed by Jang and Choi [14]. This model can improve manufacturing of nanotechnology-based coolants. Kuznetsov and Nield [15] studied a natural convective boundary layer flow of a nanofluid past an infinite vertical plate by considering thermophoresis and the Brownian motion of nanoparticles. Chamkha and Aly [16] investigated an MHD free convection flow of a nanofluid past a vertical plate in the presence of heat generation or absorption effects. In both of the above-mentioned cases [15, 16], only steady-state effects were considered. Nield and Kuznetsov [17] studied the Cheng–Minkowycz problem for a natural convection boundary layer flow in a porous medium saturated by a nanofluid. Khan and Pop [18] reported a boundary layer flow of a nanofluid past a stretching sheet. Hamad et al. [19] investigated magnetic field effects on a free convection flow of a nanofluid past a semi-infinite vertical flat plate. Recently, an unsteady boundary layer flow of a nanofluid over a permeable stretching/shrinking sheet was theoretically studied by Bachok et al. [20]. Ahmed and Pop [21] studied a mixed convection boundary layer flow from a vertical flat plate embedded in a porous medium filled with a nanofluid. Lin et al. [22] investigated a natural convective boundary layer flow of a nanofluid in a vertical cavity.

In the literature, no studies have been reported so far with regard to heat generation effects on a transient free convective flow of a nanofluid past an infinite vertical plate.

The objective of this paper is to analyze heat generation effects on a transient natural convective flow of Al_2O_3, Cu, TiO_2, and Ag nanoparticles with water as a base fluid past an infinite vertical plate. The unsteadiness is caused by impulsive motion of the vertical plate.

1. MATHEMATICAL ANALYSIS

Let us consider an unsteady incompressible two-dimensional flow of a nanofluid past an impulsively started infinite vertical plate. The flow moves along the x axis directed along the vertical plate in the upward direction, and the y axis is taken normal to it (Fig. 1).

At $t' \leqslant 0$, the plate and the fluid are at the same temperature. At $t' \leqslant 0$, the plate is at rest; at $t' > 0$, it starts to move in the vertical direction with a constant velocity u_0. It is assumed that the viscous dissipation effects are neglected, and the fluid has a volumetric rate of heat generation Q_0. The plate surface is maintained at a constant temperature T_w, which is higher than the temperature of the ambient nanofluid T_∞. The fluids under consideration are water-based nanofluids, each containing four different types of nanoparticles: aluminum oxide

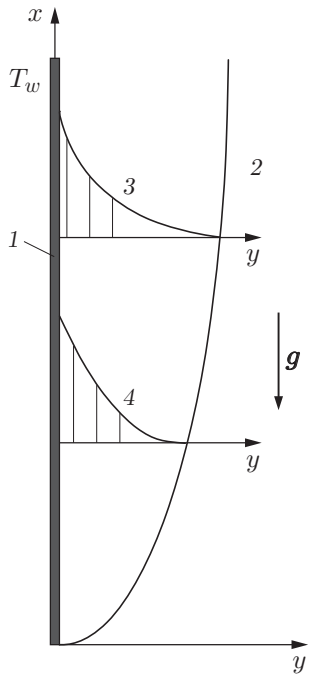

Fig. 1. Schematic diagram of the flow configuration: (*1*) vertical plate; (*2*) nanofluid; (*3*) temperature profile; (*4*) velocity profile.

Table 1. Thermophysical properties of water and nanoparticles

Nanofluid component	ρ, kg/m^3	c_p, J/(kg · K)	k, W/(m · K)
Water	997.1	4179.0	613
Al_2O_3	3970.0	765.0	40
Cu	8933.0	385.0	401
TiO_2	4250.0	686.2	8.9528
Ag	10 500.0	235.0	429

(Al_2O_3), copper (Cu), titanium oxide (TiO_2), and silver (Ag). In this case, the nanofluids are assumed to behave as single-phase fluids with a local thermal equilibrium between the base fluid and the nanoparticles suspended in it so that no slip occurs between them.

The coordinate system and the flow configuration are shown in Fig. 1. The thermophysical properties of the nanofluids are listed in Table 1 (ρ is the density, c_p is the specific heat at constant pressure, and k is the thermal conductivity) [23].

The basic unsteady momentum and thermal energy equations based on the model for nanofluids [24] satisfying the Boussinesq approximation [25] are

$$\frac{\partial u}{\partial t'} = \frac{1}{\rho_{nf}}\Big(\mu_{nf}\,\frac{\partial^2 u}{\partial y^2} + (\rho\beta)_{nf} g(T - T_\infty)\Big),$$

$$\frac{\partial T}{\partial t'} = \frac{1}{(\rho c_p)_{nf}}\Big(k_{nf}\,\frac{\partial^2 T}{\partial y^2} + Q_0(T - T_\infty)\Big). \tag{1}$$

The initial and boundary conditions are

$$t' \leqslant 0,\ u = 0,\ T = T_\infty \quad \forall\ y, \qquad t' > 0,\ u = u_0,\ T = T_w \quad \text{at} \quad y = 0,$$

$$u \to 0, \quad T \to T_\infty \quad \text{as} \quad y \to \infty. \tag{2}$$

Table 2. Models of nanofluids based on different formulas for thermal conductivity and dynamic viscosity

Model	Shape of nanoparticles	Thermal conductivity	Dynamic viscosity
1	Spherical	$\dfrac{k_{nf}}{k_f} = \dfrac{k_s + 2k_f - 2\varphi(k_f - k_s)}{k_s + 2k_f + \varphi(k_f - k_s)}$	$\mu_{nf} = \mu_f/(1-\varphi)^{2.5}$
2	Spherical	$\dfrac{k_{nf}}{k_f} = \dfrac{k_s + 2k_f - 2\varphi(k_f - k_s)}{k_s + 2k_f + \varphi(k_f - k_s)}$	$\mu_{nf} = \mu_f(1 + 7.3\varphi + 123\varphi^2)$
3	Cylindrical (nanotube)	$\dfrac{k_{nf}}{k_f} = \dfrac{k_s + k_f/2 - \varphi(k_f - k_s)/2}{k_s + k_f/2 + \varphi(k_f - k_s)}$	$\mu_{nf} = \mu_f/(1-\varphi)^{2.5}$
4	Cylindrical (nanotube)	$\dfrac{k_{nf}}{k_f} = \dfrac{k_s + k_f/2 - \varphi(k_f - k_s)/2}{k_s + k_f/2 + \varphi(k_f - k_s)}$	$\mu_{nf} = \mu_f(1 + 7.3\varphi + 123\varphi^2)$

Here u is the velocity along the x axis, ρ_{nf} is the effective density of the nanofluid, μ_{nf} is the effective dynamic viscosity of the nanofluid, β_{nf} is the thermal expansion of the nanofluid, and g is the acceleration due to gravity. For nanofluids, the expressions for ρ_{nf} and $(\rho c_p)_{nf}$ are written as

$$\rho_{nf} = (1-\varphi)\rho_f + \varphi\rho_s,$$
$$(\rho\beta)_{nf} = (1-\varphi)(\rho\beta)_f + \varphi(\rho\beta)_s, \qquad (\rho c_p)_{nf} = (1-\varphi)(\rho c_p)_f + \varphi(\rho c_p)_s. \tag{3}$$

The effective thermal conductivity of the nanofluid given by the model of Hamilton and Crosser [26] is

$$\frac{k_{eff}}{k_f} = \frac{k_s + (n-1)k_f - (n-1)\varphi(k_f - k_s)}{k_s + (n-1)k_f + \varphi(k_f - k_s)}. \tag{4}$$

In Eqs. (1)–(4), n is the empirical shape factor for the nanoparticle ($n = 3$ for spherical nanoparticles and $n = 3/2$ for cylindrical nanoparticles), φ is the solid volume fraction of nanoparticles, μ is the dynamic viscosity, and β is the thermal expansion coefficient. The subscripts nf, f, and s represent the thermophysical properties of the nanofluids, base fluid, and solid nanoparticles, respectively. The expressions for the thermal conductivity and dynamic viscosity for various models are given in Table 2.

Let us introduce the following dimensionless variables:

$$U = \frac{u}{u_0}, \qquad Y = \frac{y u_0}{\nu_f}, \qquad t = \frac{t' u_0^2}{\nu_f}, \qquad \theta = \frac{T - T_\infty}{T_w - T_\infty},$$
$$Q = \frac{Q_0 \nu_f}{u_0^2 (\rho c_p)_f}, \qquad \mathrm{Gr} = \frac{g\beta(T_w - T_\infty)\nu_f}{u_0^3}, \qquad \mathrm{Pr} = \frac{\nu_f}{\alpha_f}.$$

Here Gr is the Grashof number, Pr is the Prandtl number, and ν_f is the kinematic viscosity of the fluid.

The dimensionless governing partial differential equations (1) and boundary conditions (2) have the form

$$\frac{\partial U}{\partial t} = \frac{1}{(1-\varphi)^{2.5}} \frac{1}{1 - \varphi + \varphi\rho_s/\rho_f} \frac{\partial^2 U}{\partial Y^2} + \frac{1 - \varphi + \varphi(\rho\beta)_s/(\rho\beta)_f}{1 - \varphi + \varphi\rho_s/\rho_f} \mathrm{Gr}\theta; \tag{5}$$

$$\frac{\partial \theta}{\partial t} = \frac{1}{1 - \varphi + \varphi(\rho c_p)_s/(\rho c_p)_f} \Big(\frac{k_{nf}}{k_f} \frac{1}{\mathrm{Pr}} \frac{\partial^2 \theta}{\partial Y^2} - Q\theta \Big); \tag{6}$$

$$t \leqslant 0,\ U = 0,\ \theta = 0 \quad \forall\, Y, \qquad t > 0,\ U = 1,\ \theta = 1 \quad \text{for} \quad Y = 0,$$
$$U \to 0, \quad \theta \to 0 \quad \text{for} \quad Y \to \infty. \tag{7}$$

Let us introduce the following variables:

$$\alpha_1 = \frac{1}{(1-\varphi)^{2.5}} \frac{1}{1 - \varphi + \varphi\rho_s/\rho_f}, \qquad \alpha_2 = \frac{1 - \varphi + \varphi(\rho\beta)_s/(\rho\beta)_f}{1 - \varphi + \varphi\rho_s/\rho_f} \mathrm{Gr},$$
$$\alpha_3 = \frac{1}{1 - \varphi + \varphi(\rho c_p)_s/(\rho c_p)_f} \frac{k_{nf}}{k_f} \frac{1}{\mathrm{Pr}}, \qquad \alpha_4 = \frac{Q}{1 - \varphi + \varphi(\rho c_p)_s/(\rho c_p)_f}.$$

Now Eqs. (5) and (6) can be written as

$$\frac{\partial U}{\partial t} = \alpha_1 \frac{\partial^2 U}{\partial Y^2} + \alpha_2 \theta, \qquad \frac{\partial \theta}{\partial t} = \alpha_3 \frac{\partial^2 \theta}{\partial Y^2} - \alpha_4 \theta. \tag{8}$$

Equations (6) subjected to the boundary conditions (7) are solved by using the Laplace transform technique. The velocity U and temperature θ are obtained as

$$U = \operatorname{erfc}\Big(\frac{\eta}{\sqrt{\alpha_1}}\Big) + \frac{\alpha_2\alpha_3}{\alpha_1\alpha_4}\Big[\operatorname{erfc}\Big(\frac{\eta}{\sqrt{\alpha_1}}\Big) - \frac{\mathrm{e}^{zt}}{2}\,(A_1 + A_2) + \frac{\mathrm{e}^{zt}}{2}\,(B_1 + B_2) - \frac{1}{2}\,(C_1 + C_2)\Big],$$

$$\theta = \frac{1}{2}\Big[\exp\Big(2\eta\sqrt{\frac{\alpha_2 t}{\alpha_1}}\Big)\operatorname{erfc}\Big(\frac{\eta}{\sqrt{\alpha_1}} + \sqrt{\alpha_2 t}\Big) + \exp\Big(-2\eta\sqrt{\frac{\alpha_2 t}{\alpha_1}}\Big)\operatorname{erfc}\Big(\frac{\eta}{\sqrt{\alpha_1}} - \sqrt{\alpha_2 t}\Big)\Big], \tag{9}$$

where

$$A_1 = \exp\Big(2\eta\sqrt{\frac{zt}{\alpha_1}}\Big)\operatorname{erfc}\Big(\frac{\eta}{\sqrt{\alpha_1}} + \sqrt{zt}\Big), \qquad A_2 = \exp\Big(-2\eta\sqrt{\frac{zt}{\alpha_1}}\Big)\operatorname{erfc}\Big(\frac{\eta}{\sqrt{\alpha_1}} - \sqrt{zt}\Big),$$

$$B_1 = \exp\Big(2\eta\sqrt{\frac{(z+\alpha_4)t}{\alpha_3}}\Big)\operatorname{erfc}\Big(\frac{\eta}{\sqrt{\alpha_3}} + \sqrt{(z+\alpha_4)t}\Big),$$

$$B_2 = \exp\Big(-2\eta\sqrt{\frac{(z+\alpha_4)t}{\alpha_3}}\Big)\operatorname{erfc}\Big(\frac{\eta}{\sqrt{\alpha_3}} - \sqrt{(z+\alpha_4)t}\Big),$$

$$C_1 = \exp\Big(2\eta\sqrt{\frac{\alpha_4 t}{\alpha_3}}\Big)\operatorname{erfc}\Big(\frac{\eta}{\sqrt{\alpha_3}} + \sqrt{\alpha_4 t}\Big), \quad C_2 = \exp\Big(-2\eta\sqrt{\frac{\alpha_4 t}{\alpha_3}}\Big)\operatorname{erfc}\Big(\frac{\eta}{\sqrt{\alpha_3}} - \sqrt{\alpha_4 t}\Big),$$

$$z = \frac{-\alpha_4/\alpha_3}{1/\alpha_3 - 1/\alpha_1}, \quad \eta = \frac{Y}{2\sqrt{t}}, \quad \operatorname{erfc}(s) = 1 - \operatorname{erf}(s), \quad \operatorname{erf}(s) = \frac{2}{\sqrt{\pi}}\int\limits_0^s \mathrm{e}^{-s^2}\,ds.$$

The Nusselt number and the skin friction coefficient are found from the expressions

$$\mathrm{Nu} = -\frac{1}{2\sqrt{t}}\,\frac{k_{nf}}{k_f}\Big(\frac{\partial\theta}{\partial\eta}\Big)\Big|_{\eta=0}, \qquad C_f = \frac{1}{2\sqrt{t}}\,\frac{1}{(1-\varphi)^{2.5}}\Big(\frac{\partial U}{\partial\eta}\Big)\Big|_{\eta=0}.$$

2. RESULTS AND DISCUSSION

The dimensionless partial differential equations (5) and (6) together with the boundary conditions (7) are solved by using the Laplace transform technique for the exact solution. The calculations are performed for various values of problem parameters. The nanoparticle volume concentration is assumed to change in the range $0 \leqslant \varphi \leqslant 0.04$. Sedimentation takes place when the nanoparticle volume concentration exceeds 8%.

In this study, we consider spherical nanoparticles with the thermal conductivity and dynamic viscosity defined as

$$\frac{k_{nf}}{k_f} = \frac{k_s + 2k_f - 2\varphi(k_f - k_s)}{k_s + 2k_f + \varphi(k_f - k_s)}, \qquad \mu_{nf} = \frac{\mu_f}{(1-\varphi)^{2.5}}.$$

Nanofluids containing aluminum oxide (Al_2O_3), copper (Cu), titanium oxide (TiO_2), and silver (Ag) nanoparticles with water as a base fluid are considered. The Prandtl number of the fluid is taken to be 6.2. The velocity U and temperature θ are calculated by Eqs. (9). The results are in good agreement with those for a regular fluid without nanoparticles [3] (Fig. 2).

The transient velocity profiles U of the silver–water nanofluid ($\varphi = 0.04$) as functions of the parameter η for two time instants t and for different values of the heat generation parameter Q are shown in Fig. 3. Increasing the value of the heat generation parameter Q has a tendency to increase the thermal state of the fluid. In turn, an increase in the fluid temperature induces a flow toward the plate through the thermal buoyancy effect. The

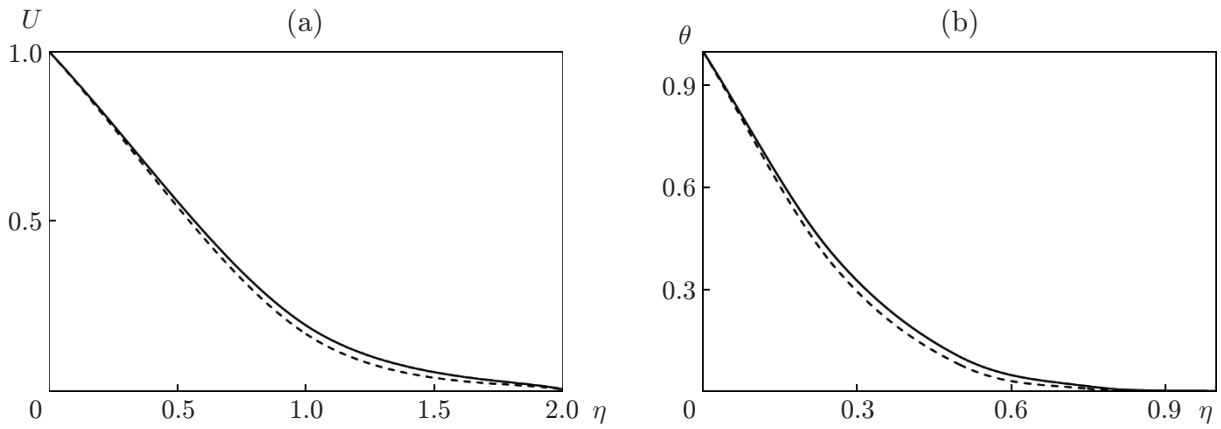

Fig. 2. Velocity U (a) and temperature θ (b) versus the parameter η for a copper–water nanofluid: the solid curves show the results of the present study ($Q = 0.2$ and $\varphi = 0.04$); the dashed curves show the data of [3] ($Q = 0$ and $\varphi = 0$).

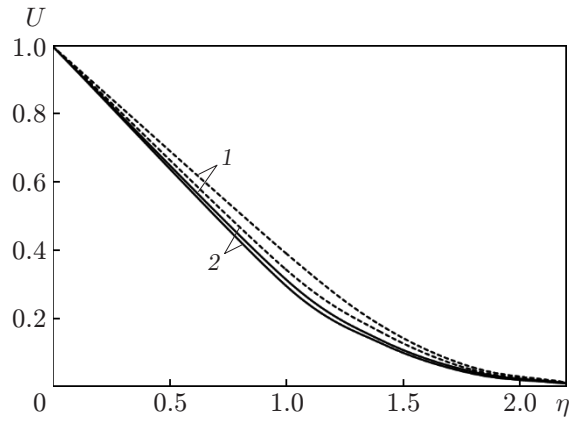

Fig. 3.

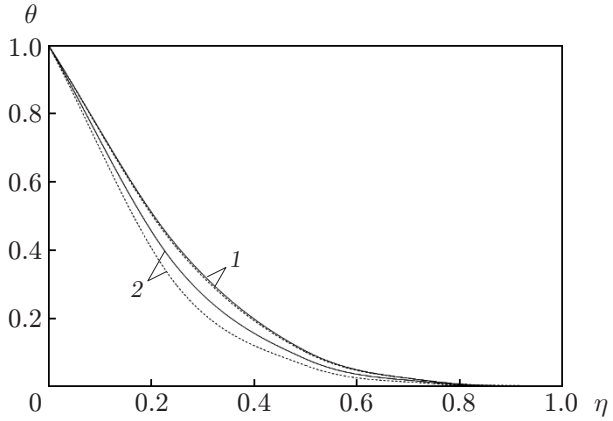

Fig. 4.

Fig. 3. Velocity U versus the parameter η for a silver–water nanofluid at Pr $= 6.2$, $\varphi = 0.04$, Gr $= 5$, and different values of Q: the solid and dashed curves show the results for $t = 0.4$ and 0.6, respectively; $Q = 0.05$ (*1*) and 0.2 (*2*).

Fig. 4. Temperature θ versus the parameter η for a silver–water nanofluid at Pr $= 6.2$, $\varphi = 0.04$, Gr $= 5$, and different values of the parameter Q: the solid and dashed curves show the results for $t = 0.2$ and 0.4, respectively; $Q = 0.2$ (*1*) and 2.0 (*2*).

momentum boundary layer thickness decreases; hence, the nanofluid velocity also decreases. It is also observed that the nanofluid velocity increases with time.

Figure 4 depicts the temperature profiles θ of the silver–water nanofluid ($\varphi = 0.04$) as a function of the parameter η for two time instants t and for different values of the heat generation parameter Q (Pr $= 6.2$ and $\varphi = 0.04$). It is observed that the temperature of the nanofluid decreases with an increase in the value of the heat generation parameter Q. As the heat generation parameter increases, more heat is produced; hence, the nanofluid velocity increases. The temperature decreases monotonically with increasing η for different values of the heat generation parameter Q and time t.

The transient velocity profiles U of the copper–water nanofluid and titanium–oxide–water nanofluid are plotted as functions of η for different values of φ in Fig. 5. With an increase in the nanoparticle volume concentration φ, the fluid velocity decreases for a fixed value of η. It is also observed that the decrease in the fluid velocity with an increase in the nanoparticle volume concentration is more pronounced for the copper–water nanofluid. This may be

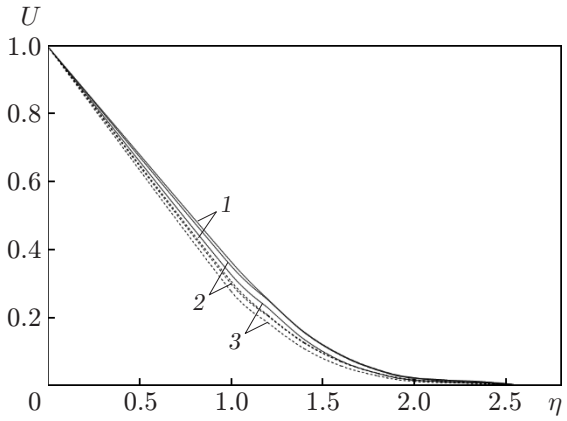

Fig. 5.

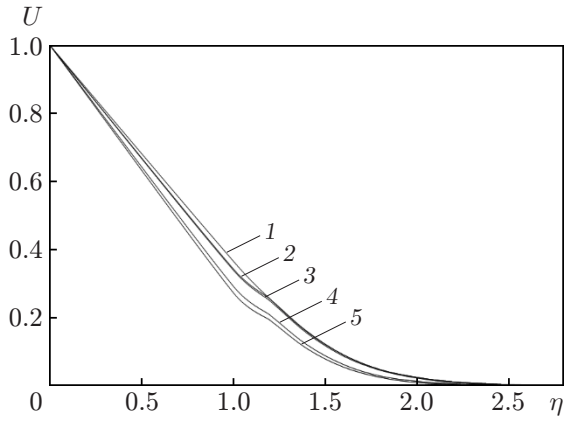

Fig. 6.

Fig. 5. Velocity U versus the parameter η at Pr $= 6.2$, $Q = 0.2$, Gr $= 5$, and different values of φ: the solid and dashed curves show the results for $t = 0.6$ and 0.4, respectively; curves *1–3* show the results for the fluid without nanoparticles ($\varphi = 0$), for the nanofluid with titanium oxide particles ($\varphi = 0.02$), and for the nanofluid with copper particles, respectively.

Fig. 6. Velocity U versus the parameter η for $\varphi = 0.04$, Gr $= 5$, $Q = 0.2$, Pr $= 6.2$, and different types of nanoparticles: fluid without nanoparticles (*1*), nanofluid with Al_2O_3 particles (*2*), nanofluid with TiO_2 particles (*3*), nanofluid with Cu particles (*4*), and nanofluid with Ag particles (*5*).

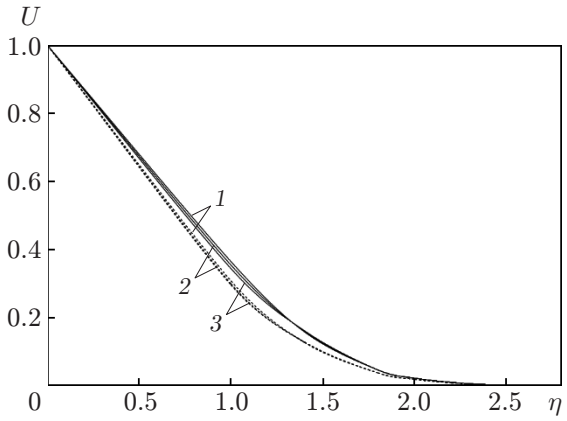

Fig. 7.

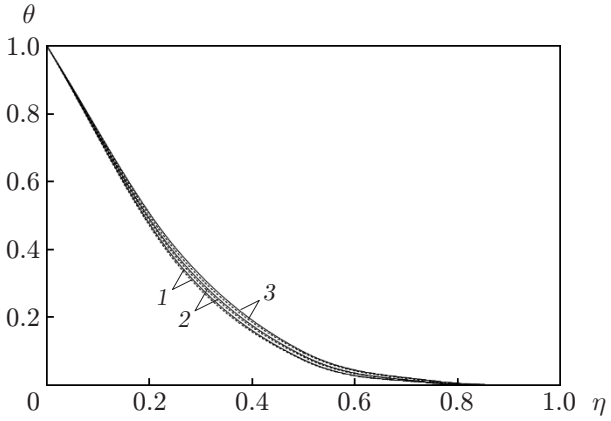

Fig. 8.

Fig. 7. Velocity U of the nanofluid with aluminum oxide particles versus the parameter η at Pr $= 6.2$, $Q = 0.2$, Gr $= 5$, and different values of the parameter φ: the solid and dashed curves show the results for $t = 0.6$ and 0.4, respectively; $\varphi = 0$ (*1*), 0.02 (*2*), and 0.04 (*3*).

Fig. 8. Temperature θ of the nanofluid with copper particles versus the parameter η at Pr $= 6.2$, $Q = 0.2$, Gr $= 5$, and different values of the parameter φ: the solid and dashed curves show the results for $t = 0.2$ and 0.4, respectively; $\varphi = 0$ (*1*), 0.02 (*2*), and 0.04 (*3*).

due to the fact that the thermal conductivity of the nanofluid depends on the nanoparticle volume concentration. It is observed that the nanofluid velocity increases with time in the presence of heat generation.

Figure 6 shows the velocity profiles U of all nanofluids as functions of the parameter η. It is observed that addition of different types of nanoparticles suppresses the velocity regardless of the type of nanoparticles. It is also noticed that the velocity of the silver–water nanofluid is smaller as compared to other nanofluids under consideration, which infers that the change in the flow velocity is associated with the thermal conductivity of nanofluids.

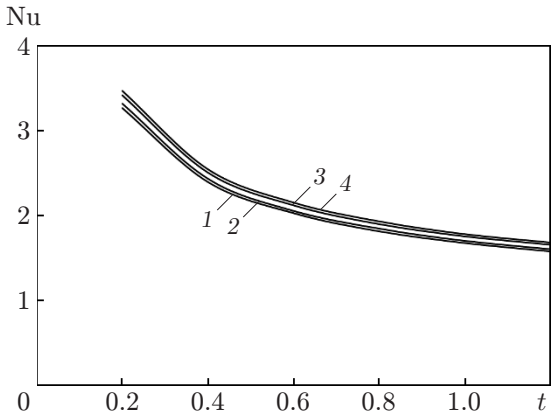

Fig. 9.

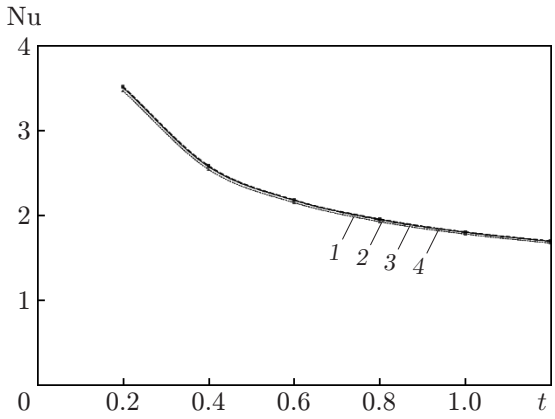

Fig. 10.

Fig. 9. Nusselt number versus time for the silver–water nanofluid at Pr = 6.2, $Q = 0.2$, Gr = 5, and $\varphi = 0$ (*1*), 0.01 (*2*), 0.02 (*3*), and 0.04 (*4*).

Fig. 10. Nusselt number versus time at Pr = 6.2, $Q = 0.2$, Gr = 5, and $\varphi = 0.04$ for nanofluids with different types of nanoparticles: nanofluid with TiO_2 particles (*1*), nanofluid with Al_2O_3 particles (*2*), nanofluid with Cu particles (*3*), and nanofluid with Ag particles (*4*).

The transient velocity profiles U of the aluminum–oxide–water nanofluid are plotted in Fig. 7 as functions of the parameter η for different volume concentrations ($\varphi = 0$, 0.02, and 0.04). It is observed that the fluid velocity is higher in the absence of nanoparticles than the nanofluid velocity. The velocity is found to increase with time.

Figure 8 shows the effect of the nanoparticle volume concentration η on the temperature profile θ of the copper–water nanofluid for $\varphi = 0$, 0.02, and 0.04. It is seen that the thermal boundary layer increases continuously with an increase in the nanoparticle volume concentration. This is due to the physical behavior of nanofluids that the thermal conductivity increases with an increase in the nanoparticle volume concentration. It is inferred from Figs. 7 and 8 that the changes in the velocity and temperature of nanofluids are associated with the change in the nanoparticle volume concentration. This suggests the use of nanofluids in processes that involve heat transfer.

Figure 9 shows that the rate of heat transfer increases with an increase in the nanoparticle volume concentration in the range $0 \leqslant \varphi \leqslant 0.04$ owing to the higher thermal conductivity of nanofluids. The greater the nanoparticle volume concentration, the greater the heat transfer rate, which is an important feature of nanofluids.

The nanofluid properties vary significantly within the boundary layer because of the temperature gradient. The effect of the temperature gradient can result in a significant decrease in viscosity and, thus, enhance the heat transfer. The heat transfer rate is more pronounced in the silver–water nanofluid than in the other nanofluids (Fig. 10). This is due to the fact that silver (Ag) nanoparticles have the highest thermal conductivity among all types of nanoparticles under consideration.

It is observed from Fig. 11 that the skin friction coefficient C_f increases with an increase in the nanoparticle volume concentration. As the time increases, the skin friction coefficient decreases and becomes negative, which shows that a reverse type of the flow occurs near the plate. Thus, the presence of nanoparticles results in an increased magnitude of skin friction.

CONCLUSIONS

The present analysis investigates an unsteady natural convective flow of a nanofluid past an infinite vertical plate with heat sources. The dimensionless partial differential equations are solved by using the Laplace transform technique. The velocity and temperature profiles of different types of nanofluids with different nanoparticle volume concentrations are studied. The expressions for the Nusselt number and skin friction coefficient are also obtained.

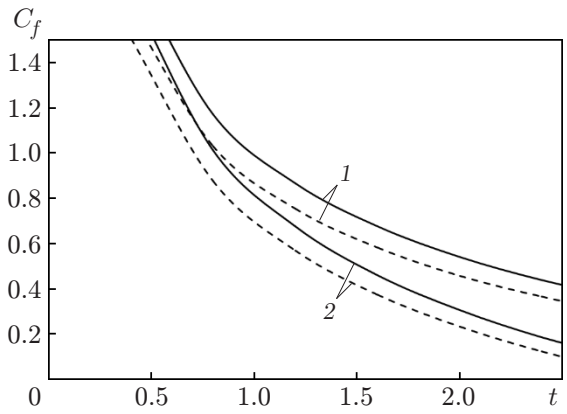

Fig. 11. Skin friction coefficient versus time for the copper–water nanofluid for Pr = 6.2 and different values of Gr: the solid and dashed curves show the results for $\varphi = 0.04$ and 0, respectively; Gr = 0.3 (*1*) and 0.5 (*2*).

The conclusions of this study can be summarized as follows. An increase in the nanoparticle volume concentration φ yields an increase in the nanofluid temperature, which leads to an increase in the heat transfer rate. An increase in the nanoparticle volume concentration φ leads to an increase in the skin friction coefficient. An increase in the heat generation parameter decreases the temperature and velocity of the nanofluid. The silver–water nanofluid is proved to have a higher heat transfer rate than the nanofluids containing copper, aluminum oxide, and titanium oxide particles.

REFERENCES

1. S. U. S. Choi, "Enhancing Thermal Conductivity of Fluids with Nanoparticles," in *Developments and Applications of non-Newtonian Flows* (Amer. Soc. Mech. Eng., New York, 1995), Vol. 231, pp. 99–105.
2. G. G. Stokes, "On the Effects of Internal Friction of Fluids on the Motion of Pendulums," Cambridge Philos. Trans. **9**, 8–106 (1851).
3. V. M. Soundalgekar, "Free Convection Effects on the Stokes Problem for an Infinite Vertical Plate," Trans. ASME, J. Heat Transfer **99** (3), 499–501 (1977).
4. A. A. Raptis and G. J. Tzivanidis, "Effects of Mass Transfer, Free-Convection Currents and Heat Sources on the Stokes Problem for an Infinite Vertical Plate," Astrophys. Space Sci. **78** (2), 351–357 (1981).
5. H. Masuda, A. Ebata, K. Teramae, and N. Hishinuma, "Alteration of Thermal Conductivity and Viscosity of Liquid by Dispersing Ultra-Fine Particles. Dispersion of C-Al_2O_3, SiO_2 and TiO_2 Ultra-Fine Particles," Netsu Bussei **7** (4), 227–233 (1993).
6. S. Lee, S. U. S. Choi, S. Li, and J. A. Eastman, "Measuring Thermal Conductivity of Fluids Containing Oxide Nanoparticles," Trans. ASME, J. Heat Transfer **121** (2), 280–289 (1999).
7. Y. Xuan and Q. Li, "Heat Transfer Enhancement of Nanofluids," Int. J. Heat Fluid Flow **21**, 58–64 (2000).
8. Y. Xuan and W. Roetzel, "Conceptions for Heat Transfer Correlation of Nanofluids," Int. J. Heat Mass Transfer **43** (19), 3701–3707 (2000).
9. J. A. Eastman, S. U. S. Choi, S. Li, et al., "Anomalously Increased Effective Thermal Conductivity of Ethylene Glycol-Based Nanofluids Containing Copper Nanoparticles," Appl. Phys. Lett. **78** (6), 718–720 (2001).
10. B. C. Pak and Y. I. Cho, "Hydrodynamic and Heat Transfer Study of Dispersed Fluids with Submicron Metallic Oxide Particles," Exp. Heat Transfer **11** (2), 151–170 (1998).
11. J. Buongiorno, "Convective Transport in Nanofluids," Trans. ASME, J. Heat Transfer **128** (3), 240–250 (2006).
12. D. Wen and Y. Ding, "Natural Convective Heat Transfer of Suspensions of Titanium Dioxide Nanoparticles (Nanofluids)," IEEE Trans. Nanotechnol. **5** (3), 220–227 (2006).
13. L. Gosselin and A. K. Da Silva, "Combined Heat Transfer and Power Dissipation Optimization of Nanofluid Flows," Appl. Phys. Lett. **85** (18), 4160–4162 (2004).

14. S. P. Jang and S. U. S. Choi, "Role of Brownian Motion in the Enhanced Thermal Conductivity of Nanofluids," Appl. Phys. Lett. **84** (21), 4316–4318 (2004).
15. A. V. Kuznetsov and D. A. Nield, "Natural Convective Boundary-Layer Flow of a Nanofluid Past a Vertical Plate," Int. J. Thermal. Sci. **49** (2), 243–247 (2010).
16. A. J. Chamkha and A. M. Aly, "MHD Free Convection Flow of a Nanofluid Past a Vertical Plate in the Presence of Heat Generation or Absorption Effects," Chem. Eng. Comm. **198**, 425–441 (2011).
17. D. A. Nield and A. V. Kuznetsov, "The Cheng–Minkowycz Problem for Natural Convective Boundary-Layer Flow in a Porous Medium Saturated by a Nanofluid," Int. J. Heat Mass Transfer **52** (25/26), 5792–5795 (2009).
18. W. A. Khan and I. Pop, "Boundary-Layer Flow of a Nanofluid Past a Stretching Sheet," Int. J. Heat Mass Transfer **53** (11/12), 2477–2483 (2010).
19. M. A. A. Hamad, I. Pop, and A. I. Md. Ismail, "Magnetic Field Effects on Free Convection Flow of a Nanofluid Past a Vertical Semi-Infinite Flat Plate," Nonlinear Anal. Real World Appl. **12** (3), 1338–1346 (2010).
20. N. Bachok, A. Ishak, and I. Pop, "Unsteady Boundary-Layer Flow and Heat Transfer of a Nanofluid Over a Permeable Stretching/Shrinking Sheet," Int. J. Heat Mass Transfer **55** (7/8), 2102–2109 (2012).
21. S. Ahmed and I. Pop, "Mixed Convective Boundary Layer Flow from a Vertical Flat Plate Embedded in a Porous Medium Filled with Nanofluids," Int. Comm. Heat Mass Transfer **37** (8), 987–991 (2010).
22. K. C. Lin and A. Violi, "Natural Convection Heat Transfer of Nanofluids in a Vertical Cavity: Effects of Non-Uniform Particle Diameter and Temperature on Thermal Conductivity," Int. J. Heat Fluid Flow **31** (2), 236–245 (2010).
23. H. F. Oztop and E. Abu-Nada, "Numerical Study of Natural Convection in Partially Heated Rectangular Enclosures Filled with Nanofluids," Int. J. Heat Fluid Flow **29** (5), 1326–1336 (2008).
24. R. K. Tiwari and M. K. Das, "Heat Transfer Augment in a Two-Sided Lid-Driven Differentially Heated Square Cavity Utilizing Nanofluids," Int. J. Heat Mass Transfer **50** (9/10), 2002–2018 (2007).
25. H. Schlichting and K. Gersten, *Boundary Layer Theory* (Springer-Verlag, Berlin, 2001).
26. R. L. Hamilton and O. K. Crosser, "Thermal Conductivity of Heterogeneous Two-Component Systems," Indust. Eng. Chem. Fundament. **1** (3), 187–191 (1962).